ADVANCED FUNCTIONAL MATERIALS

FULL PAPER

The Preparation and Characterization of Small Mesopores in Siloxane-Based Materials That Use Cyclodextrins as Templates

By *Jin-Heong Yim*,* *Yi-Yeol Lyu*, *Hyun-Dam Jeong*, *Se Ahn Song, Il-Sun Hwang*, *Jingyu Hyeon-Lee*, *Sang Kook Mah*, *Seok Chang*, *Jae-Geun Park*, *Yifan F. Hu*, *Jianing N. Sun*, and *David W. Gidley*

Porous thin films containing very small closed pores (~20 Å) with a low dielectric constant (~2.0) and excellent mechanical properties have been prepared using the mixture of cyclic silsesquioxane (CSSQ) and a new porogen, heptakis(2,3,6-tri-*O*-methyl)-β-cyclodextrin (tCD). The pore sizes vary from 16.3 Å to 22.2 Å when the content of tCD in the coating mixture increases to 45 wt.-% according to positronium annihilation lifetime spectroscopy (PALS) analysis. It has also been found that the pore percolation threshold (the onset of pore interconnectivity) occurs as the ~50 % tCD porogen load. The dielectric constants ($k = 2.4 \sim 1.9$) and refractive indices of these porous thin films decreased systematically as the amount of porogen loading increased in the coating mixture. The electrical properties and mechanical properties of such porous thin films were fairly good as interlayer dielectrics.

1. Introduction

Porous materials with ordered micropores (typically less than 1 nm) such as zeolites have been used widely as catalysts, adsorbent, and various supporting materials.[1] Recently, some research has been performed in the syntheses of new porous materials extending the pore diameter to the mesoporous region (typically 1.6 ~ 30 nm).[2] The pore size and pore-size distribution could be tuned by using different types of pore templates and reaction conditions. Especially, Antonietti and co-workers have reported that cyclodextrins can act as templates for the production of porous silica materials with pore sizes exactly resembling the cyclodextrin diameters(1.5 ~ 2 nm) and a bicontinuous "worm-type" pore structure using a nanocasting concept.[3]

Thin films using porous materials have potential applications in the field of sensors, waveguides, etc. In particular, many porous thin films were developed as low-*k* materials as interlayer dielectrics in large-scale integrated circuits (LSI).[4] A simpler way to prepare porous thin films has been developed by spin coating and dip coating etc. The spin-coating method seems to be more attractive as compared to the dip-coating method from the industrial point view. We introduce herein a cyclodextrin as a pore template material for producing porous thin films by using a simple spin-coating method.

[*] Dr. J.-H. Yim, Y.-Y. Lyu, Dr. H.-D. Jeong, I.-S. Hwang, Dr. J. Hyeon-Lee, Dr. S. K. Mah, Dr. S. Chang, Dr. J.-G. Park
E-Polymer Lab., Samsung Advanced Institiue of Technology (SAIT)
San 14-1, Nongseo-ri, Kiheung-eup
Yongin-shi, Kyungki-do, 449-712 (Korea)
E-mail: ch20889@sait.samsung.co.kr

Dr. S. A. Song
AE Center, Samsung Advanced Institiue of Technology (SAIT)
San 14-1, Nongseo-ri, Kiheung-eup
Yongin-shi, Kyungki-do, 449-712 (Korea)

Dr. Y. F. Hu, Dr. J. Sun, Prof. D. W. Gidley
Department of Physics, University of Michigan
Ann Arbor, MI 48109 (USA)

Cyclodextrins are cyclic oligosaccharides consisting of at least six glucopyranose units that are joined together by an $\alpha(1 \longrightarrow 4)$ linkage. The initial discovery of cyclodextrins is attributed to Villers, who isolated them as degradation products of starch.[5] X-ray crystallographic studies have firmly established the relationship between the structure and stereochemistry of cyclodextrin.[6] The six-glucose unit containing cyclodextrin is specified as α-cyclodextrin, while the cyclodextrins with seven and eight glucose units are designated as β-cyclodextrin and γ-cyclodextrin, respectively. These cyclodextrin compounds have three-dimensional structure with maximum diameter of 13.7 ~ 16.9 Å. In addition, cyclodextrin compounds can be easily modified by functionalization of their reactive hydroxyl groups.[5] We consider cyclodextrins as promising pore templates (porogen) due to their many desirable properties, such as small molecular size (14 ~ 17 Å), compatible with siloxane-based matrix precursors (with reactive Si–OH groups), narrow decomposition temperature window (< 100 °C), and low cost.

The purpose of our work is to make siloxane-based porous thin films with small mesopores (~20 Å) templated by cyclodextrin. In order to know the decomposition behaviors of cyclodextrin, thermogravimetric analysis (TGA) and in-situ FTIR studies were performed. Pore size, porosities, and distributions of the porous thin films were investigated by means of N_2 sorption, positronium annihilation lifetime spectroscopy (PALS), Rutherford backscattering spectroscopy (RBS), and transmission electron microscopy (TEM). We have also monitored the electrical properties, including dielectric constant and leakage current, and mechanical properties such as hardness and modulus of the porous thin films to evaluate their performance as interlayer dielectric materials in LSI devices.

2. Results and Discussion

In this study, we use CSSQ (cyclic silsesquioxane) as a matrix precursor. CSSQ was prepared by acid-catalyst controlled

  DOI: 10.1002/adfm.200304287

hydrolytic polycondensation of 2,4,6,8-tetramethyl-2,4,6,8-tetra(trimethoxysilylethyl)cyclotetrasiloxane.[7] The mechanical properties of the cured CSSQ film, such as hardness (~7 GPa), modulus(~1.2 GPa), and crack-free thickness (<2) were excellent as compared to the previous silsesquioxane- (SSQ)-based spin-on glass (SOG) type low-*k* materials.

In order to know the structural changes of heptakis(2,3,6-tri-O-methyl)-*β*-cyclodextrin (tCD) and thin films made from mixture of CSSQ and tCD as a function of temperature, FTIR spectra were collected at increasing temperature under a nitrogen atmosphere as shown in Figure 1. The characteristic

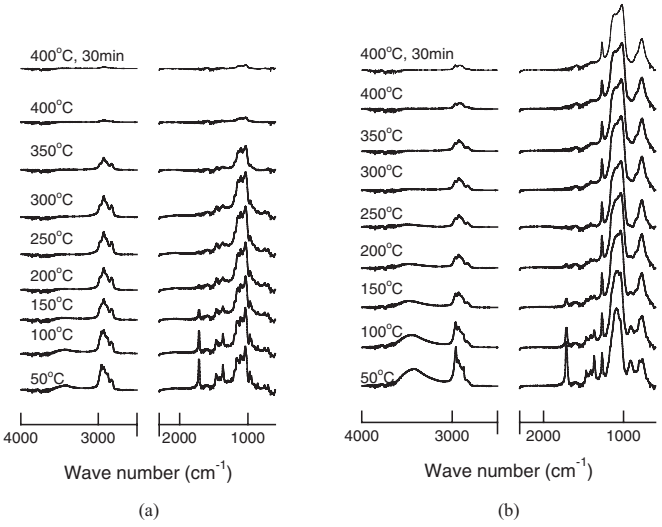

Fig. 1. Temperature sweep in-situ FTIR spectra of a) tCD and b) CSSQ/tCD mixture (content of tCD = 28.5 wt.-%).

peak in the 4-methyl-2-pentanone as a solvent is a carbonyl group-(C=O) peak, which is located at 1718 cm^{-1}. This peak completely disappeared at 200 °C, indicating the solvent has been removed. Aliphatic stretching peaks (C–H) and ether (C–O–C) linkages in tCD, characterized by peaks at 2800 ~ 3000, and 1000 ~ 1250 cm^{-1}, respectively, start to change at 350 °C. This means that the structure of tCD remains unchanged up to 350 °C, before decomposing at higher temperatures. Hydroxyl groups such as –OH and Si–OH with signals found at 3400 cm^{-1} and 910 cm^{-1}, respectively, mainly come from the CSSQ precursor. The height of these peaks decreased as a function of temperature due to polycondensation reaction of the precursor molecules. It seems that the polycondensation is almost completed at 300 °C, as reported previously.[8] Therefore, tCD could be used as a porogenic material, because its three-dimensional structure can be sustained until the completion of vitrifying the CSSQ matrix.

Figure 2 shows the results of thermogravimetric analysis (TGA) of tCD, CSSQ precursor, and the films made from a mixture of CSSQ and tCD containing 18.7 and 28.5 wt.-% tCD. The weight of CSSQ precursor decreases about 11 % due to the crosslinking reaction of residual Si–OH groups in the precursor up to 300 °C. And there was almost no weight loss at the CSSQ precursor above 300 °C. In the case of tCD, major

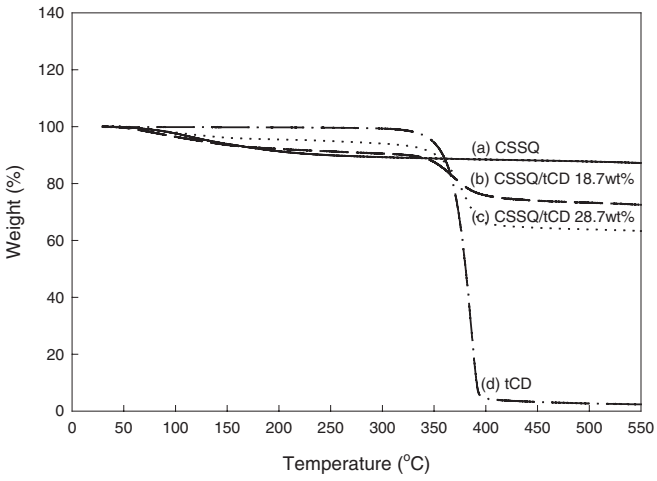

Fig. 2. Comparisons of thermogravimetric analysis (TGA) data for a) tCD, b) CSSQ, c) CSSQ/tCD 18.7 wt.-%, and d) CSSQ/tCD 28.7 wt.-%.

decomposition occurred between 320 °C and 392 °C, as shown in Figure 2.

These TGA results are consistent with in-situ FTIR results. The decomposition temperature range in the films made from a mixture of CSSQ and tCD was almost the same as that of tCD alone. This means that there was almost no influence of the surrounding inorganic matrix on the decomposition behavior of tCD. Moreover, the decomposition window of tCD was much narrower than that of the star-shaped poly(caprolactone)-based dendrimer that was reported as a porogenic material.[9]

It was difficult to detect the pores that exist in the CSSQ–tCD films by means of TEM. No pore structure was detected in the thin films made from the mixture of CSSQ and tCD with the tCD content up to 50 %, as shown in Figure 3. Although

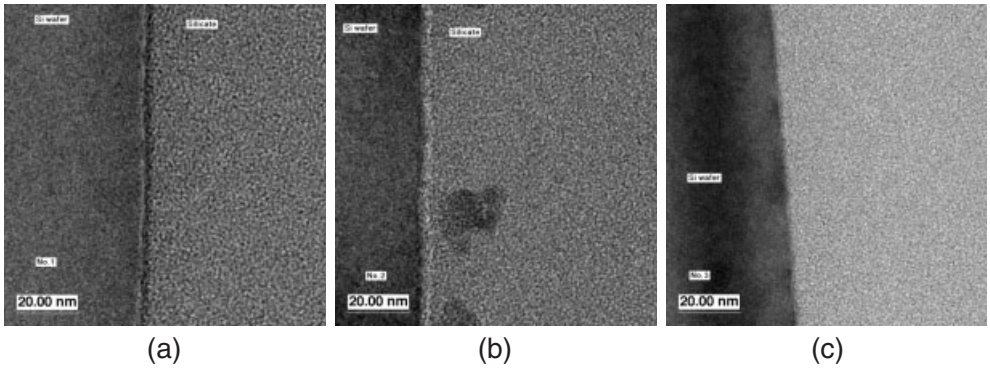

Fig. 3. Comparisons of TEM images as a function of content of tCD weight percent a) CSSQ, b) CSSQ/tCD 30 wt.-%, c) CSSQ/tCD 50 wt.-%.

the pores made from the well-dispersed single molecules of tCD were not observed yet by TEM, it can be predicted that there is no detectable agglomeration of tCD molecules in the siloxane matrix and the pores of thin films are homogeneously distributed, very probably in single-molecule dispersion.

As shown in Table 1, average pore diameter, pore volume, and surface area, which are measured by N_2 sorption experiment, increased as a function of content of tCD, systematically. It was postulated that an aggregation of tCD was not significant, because the average pore size of films with 50 % tCD was only 21.1 Å. The pore size was calculated by the Brunauer–Emmett–Teller (BET) method from the desorption isotherm of N_2. One peak around 15 ~ 16 Å was detected in the pore-size distribution curve of all of the prepared films. Figure 4 shows typical examples of pore-size distribution curves of films made from mixture of CSSQ and tCD (30 % and 50 %). Considering the maximum radius of β-type cyclodextrin is about 15 Å, it is interesting that the size of a peak in the pore-size distribution curve is similar to the size of β-type cyclodextrin. Therefore, we think that most of the pores are each generated from a single tCD molecule.

Table 1. Pore diameter, pore volume, and surface area of porous powder samples as a function of cyclodextrin contents.

tCD Content [wt.-%] [a]	Average pore diameter[Å] [c]	Pore volume [cm^3/g] [b]	Surface area [m^2/g] [c]
10	11.4	0.150	207
20	16.9	0.180	483
30	17.0	0.220	522
40	19.6	0.370	593
50	21.1	0.380	634

[a] Porous powders were obtained by decompose of tCD in the mixture of CSSQ/tCD. [b] Calculated by BJH method. [c] Calculated by the BET method.

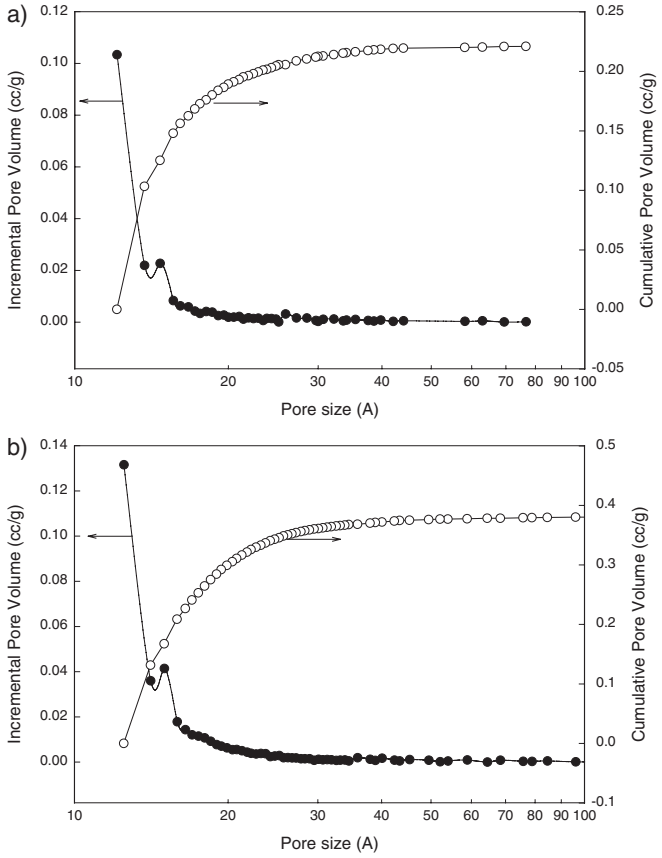

Fig. 4. Typical pore-size distribution curves of calcinated samples from mixture of a) CSSQ/tCD 30 wt.-% and b) CSSQ/tCD 50 wt.-%.

PALS has been used to measure the pore size and to elucidate the nature of the pore structure, i.e., closed or open pores. The non-porous CSSQ film was investigated to probe the voids in the host matrix. Two very short positronium (Ps) lifetimes of about 2 ns and 6 ns were required in fitting the spectra. Such lifetimes correspond to pore diameters in the 6–10 Å range, and such sub-nanometer pores will be referred to as "micropores". These pores are closed and isolated and there could be a size distribution within this range. Further analysis to define the pore-size distribution[10] will not be discussed. These closed micropores, intrinsic to the dense CSSQ matrix, are detected in all of the porous films. Other than these micropores, bigger pores are detected in the porous films as indicated by longer Ps lifetime components (Table 2). It is found that the pore size depends on the loading of tCD in the mixture, varying in diameter[11] from 16.3 ± 0.3 Å (10 % tCD) to 22.2 ± 0.4 Å (45 % tCD), as shown in Table 2. These values correspond to the average spherical pore diameters of the closed pores in these films.

Table 2. Pore size and types of pore for the porous thin films as a function of cyclodextrin contents. Lifetime values were averaged from data acquired at 3, 5, and 8 keV.

Sample [a]	O-Ps Lifetime [ns]	Pore diameter [Å]	Remarks
CSSQ	2.0 and 6.0	6 and 10	micropore
CSSQ/tCD 10 %	15.0~16.0	16.3 ± 0.3	Closed pore
CSSQ/tCD 30 %	21.3	19.2 ± 0.3	Closed pore
CSSQ/tCD 35 %	23.9	20.4 ± 0.3	Closed pore
CSSQ/tCD 40 %	25.3	21.0 ± 0.2	Closed pore
CSSQ/tCD 45 %	27.6	22.2 ± 0.2	Closed pore
CSSQ/tCD 50 %	25.0	21.5 ± 0.2	Slightly open
CSSQ/tCD 55 %	29.3	23.2 ± 0.2	Open pore
CSSQ/tCD 60 %	28.6	23.0 ± 0.3	Open pore

[a] The procedures of thin-film sample preparation is explained in the Experimental section.

In addition to pore size, it is important to know the pore interconnectivity, which may affect the overall film properties. Large and interconnected pores, for instance, will make the film more susceptible to metal diffusion and contamination. Pore interconnectivity can easily be determined from Ps vacuum signal in PALS spectra. Ps formed in the films can escape to vacuum if the pores are interconnected and open paths to the vacuum are formed. We have noticed that some Ps is able to escape into the vacuum system (decaying with the vacuum lifetime of ~ 140 ns) with the sacrifice of Ps intensity in the films when the porogen percentage goes above 50 %, as shown in Figure 5. It indicates that the isolated pores, increasing in size as the porogen loading goes up (Table 2), have eventually become interconnected. The onset of pore interconnectivity, the so-called pore-percolation threshold in these films, occurs near 50–55 % porogen loading. Note the pores are still very small even at high porogen loadings. It means that the pores

ADVANCED FUNCTIONAL MATERIALS

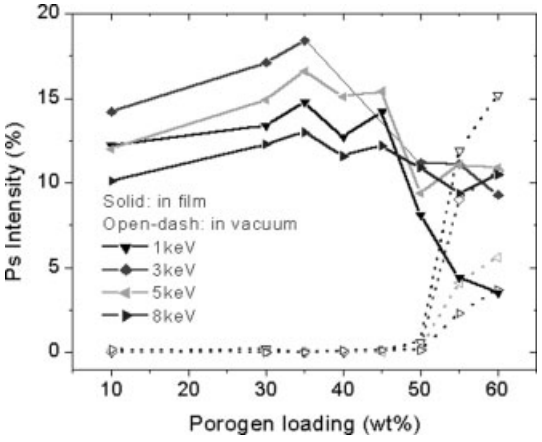

Fig. 5. Ps intensity as a function of porogen loading. The Ps vacuum intensity represents the Ps escaped from the film. The Ps film intensity includes Ps that annihilated in both micro- and mesopores.

tend to widely spread within the matrix material instead of agglomerating into big ones. This probably explains the high percolation threshold (50 %) observed in these films. Antonietti and co-workers reported that the pore structure of porous silica materials that were made from hydrophilic cyclodextrins in aqueous solution as template show a "worm-like" pore system.[3] Considering their results, the interconnected pore structure of the CSSQ/tCD system, which contains high porogen loading (> 50 %) might also be a "worm-like" pore structure. However, the single-molecule isolated pore could be generated in the CSSQ/tCD system under the dilute tCD loading (< 40 %).

The refractive index decreased as expected and the porosity increased as a function of content of tCD in the mixture as shown in Table 3. The porosities of thin films were calculated using Equation 1

$$\text{Porosity} = (1-\rho_p/\rho_m) \times 100 \quad (1)$$

where ρ_p = density of porous film, and ρ_m = density of non-porous film of CSSQ. The porosity of the thin film was much lower than the content of tCD in the coating mixtures for high porogen loads (above 40 %). Pore collapse might have occurred during decomposition of tCD in these samples. Despite this, closed pore structures were still retained based on PALS results.

Table 3. The variation of refractive index and porosity of porous thin films as a function of cyclodextrin contents.

Sample	Refractive index [a]	Density [b] [g cm^{-3}]	Porosity [c]
CSSQ	1.433	1.447	–
CSSQ/tCD 10 %	1.398	1.311	9.4
CSSQ/tCD 20 %	1.367	1.216	16.0
CSSQ/tCD 30 %	1.353	1.114	23.0
CSSQ/tCD 40 %	1.335	1.073	25.9
CSSQ/tCD 50 %	1.315	1.017	29.7

[a] Refractive index and thickness measured by prism coupler. [b] Film density measured by RBS with 3.6 MeV $^4He^+$ ion. [c] Porosities were calculated using Equation 1.

The electrical properties such as dielectric constant and mechanical properties such as hardness and modulus were summarized in Table 4. The dielectric constant of the porous thin film made from tCD varied from 2.4 to 1.9 as tCD content increases from 10 to 50 wt.-%. Leakage current was determined to be on the order of 10^{-10} A cm^{-2}, which should be acceptable for the application to LSI devices because SiOF films ($k \approx 3.5$), with leakage current density on the order of 10^{-10} A cm^{-2}, have been used widely in real LSI devices in recent years.[12] The hardness and modulus of porous thin films made with 30 % of tCD were also fairly good as prospective interlayer dielectrics. The electrical properties and mechanical properties of porous thin films from tCD do not change abruptly, even though porogen content increases up to 50 %. It might be related to the high percolation threshold (~ 50 %) in such a CSSQ/tCD system.

Table 4. The electrical properties and mechanical properties of porous thin films as a function of cyclodextrin contents.

Sample	Electrical properties		Mechanical properties [a]	
	Dielectric constant [k]	Leakage current [A cm^{-2} @0.4MV]	Hardness [GPa]	Modulus [GPa]
CSSQ	2.51	6.9 x 10^{-11}	1.19	7.14
CSSQ/tCD 10 %	2.38	1.1 x 10^{-10}	0.73	4.62
CSSQ/tCD 30 %	1.98	2.5 x 10^{-10}	0.60	4.51
CSSQ/tCD 50 %	1.90	2.0 x 10^{-10}	0.44	3.71

[a] Mechanical properties were measured by nanoindentation, and hardness and elastic modulus of all films were collected at the indentation depth of 50 nm.

3. Conclusion

In conclusion, the nanoporous polysiloxane-based thin films were successfully prepared with heptakis(2,3,6-tri-*O*-methyl)-β-cyclodextrin (tCD) as a template material. The small molecular size of tCD and narrow thermal decomposition window (320 ~ 390 °C) results in small nanopores which grow only slightly in size as the tCD content increases. The pores are closed, and their diameter varies from 16.3 Å to 22.2 Å when the content of tCD in the coating mixture reaches 45 %. The dielectric constants and refractive indexes of the thin films decreased as the amount of porogen loading increased in the coating precursors. The electrical properties and mechanical properties of porous thin films obtained from the mixture of cyclic silsesquioxane (CSSQ) and tCD show good potential as interlayer dielectrics.

4. Experimental

2,4,6,8-Tetramethyl-2,4,6,8-tetravinylcyclotetrasiloxane (Aldrich) was used as received. Catalysts such as hydrochloric acid (Samchun Pure Chemical Co.), platinum (*O*)-1,3-divinyl-1,1,3,3-tetramethyldisiloxane complex in xylene (Aldrich) were also used as received. Triethylamine (Aldrich), anhydrous sodium sulfate (Samchun Pure Chemical Co.), methyl alcohol (Aldrich), and 4-methyl-2-pentanone (Aldrich), heptakis(2,3,6-tri-*O*-methyl)-β-cyclodextrin were used as received without further purification. Solvents such as tetrahydrofuran (J. T. Baker), diethyl ether (J. T. Baker), and acetone (J. T. Baker) were purified by distillation in the presence of sodium under an N_2 atmosphere.

Synthesis of 2,4,6,8-tetramethyl-2,4,6,8-tetra(trimethoxysilylethyl)cyclotetrasiloxane (TCS): To a flask were added 29.014 mmol (10.0 g) 2,4,6,8-tetramethyl-2,4,6,8-tetravinylcyclotetrasiloxane and 0.164 g platinum (*O*)-1,3-divinyl-1,1,3,3-tetramethyldisiloxane complex (solution in xylene), which were then diluted with 300 mL diethyl ether. Next, the flask was cooled to –78 °C, 127.65 mmol (17.29 g) trichlorosilane was slowly added thereto, and then it was slowly warmed to room temperature. The reaction was continued at room temperature for 48 h, and any volatile materials were removed from the reaction mixture under a reduced pressure of about 0.1 torr. 23.1 g of a brown liquid compound, $[–Si(CH_3)(CH_2CH_2Cl_3)O–]_4$ in a yield of 90 % were prepared.

11.28 mmol (10.0 g) of the compound was diluted with 300 mL tetrahydrofuran, and the flask was cooled to –78 °C, 136.71 mmol (13.83 g) triethylamine, and 136.71 mmol (4.38 g) methyl alcohol was added thereto, and it was slowly warmed again to room temperature. The reaction was continued at 50 °C for 15 h, filtered through celite to remove triethylamine hydrochloride salts, and then volatile materials were evaporated from the filtrate under a reduced pressure of about 0.1 torr. Subsequently, 50 mL pentane was added thereto and stirred for 1 h, and then the mixture was filtered through celite to provide a clear colorless solution. The pentane was evaporated from this solution under a reduced pressure of about 0.1 torr to afford 8.74 g of a monomer, a colorless liquid in a yield of 94 %: ^{1}H NMR (300 MHz, Acetone-d^6) δ: 0.13 (s, 12H), 0.54 ~ 0.64 (m, 16H), 3.54 (s, 36H); ^{13}C NMR (300 MHz, Acetone-d^6) δ: –1.84 ($D_2^{(CH3)}$), 0.74 ($T_0^{(CH2)}$), 8.29 ($D_2^{(CH2)}$), 50.15 ($–OCH_3$); ^{29}Si NMR (300MHz, Acetone-d^6) δ –42.20 (T_0), –19.75 (D_2)

Polymerization of CSSQ Precursor: To a flask was added 10.80 mmol (9.00 g) TCS monomer, which was then diluted with 90 mL tetrahydrofuran. Next, diluted HCl solution (1.30 mmol hydrochloride), prepared by dilution of concentrated HCl (35 wt.-% hydrochloride) with deionized water was slowly added thereto at –78 °C, followed by addition of more deionized water, so that total amount of water including the inherent water in the above added diluted HCl solution was 431.89 mmol (7.774 g). Thereafter, the flask was slowly warmed to 70 °C, and allowed to react for 16 h. Then, the reaction mixture was transferred to a separating funnel, 180 mL diethyl ether was added thereto, and then three times washed with 50 mL deionized water. Subsequently, 5 g anhydrous sodium sulfate was added thereto and stirred at room temperature for 5 h to remove a trace of water, and then filtered out to provide a clear colorless solution. Any volatile materials were evaporated from this solution under a reduced pressure of about 0.1 torr to afford 6.3 g of crude CSSQ precursor as white powder. After dissolving the produced white power in the 5 mL of tetrahydrofuran, this solution was purified by re-precipitation with deionized water. After dissolving the produced white powder in the 5 mL of acetone, residual particles were eliminated by using membrane filter (0.2 μm). The acetone was evaporated from the solution under a reduced pressure of about 0.1 torr to afford 5.7 g of CSSQ precursor as white powder.

The microstructures of the precursors were analyzed by means of ^{1}H NMR (Bruker AM300. Based on ^{1}H NMR analysis, the Si–OH mole percentage in the prepared CSSQ precursor was calculated to be 35 % using Equation 1. Molecular weight and molecular-weight distribution of the precursors were measured by gel permeation chromatography (Waters). The weight-average molecular-weight of the CSSQ precursor was determined to be 18 900 and the molecular-weight distribution was 2.76.

$$\text{Si-OH}\,[\%] = \text{Area(Si-OH)}/[\text{Area(Si-OH)} + \text{Area(Si-OCH}_3)/3 + \text{Area(Si-CH}_3)/3] \times 100 \quad (2)$$

Preparations of Porous Thin Films: The precursor solutions were prepared by mixing the siloxane–silsesquioxane hybrid polymer, heptakis(2,3,6-tri-*O*-methyl)-β-cyclodextrin and 4-methyl-2-pentanone (MIBK) (stoichiometrically). The mixture was spin-cast at 3000 rpm for 13 s onto silicon wafers. The wafers were then subjected to a series of soft bakings on a hot plate, including 1 min at 150 °C and another minute at 250 °C to remove the organic solvent. The wafers were then cured in a cylindrical furnace (Linberg type 55642) at 420 °C for 60 min under vacuum conditions, and the porous thin films were produced.

Characterization of porous thin films: IR spectra of the precursor were recorded by FTIR (BOMEM MB-104) with in-situ heating cell under N_2 atmosphere, in order to know how the structure of precursors change according to temperature condition. Reflective index and thickness of thin films were measured by prism coupler (Metricon Co., Prism coupler 2010) and surface profiler (Tenco P-10). Film density and porosity were measured by RBS (Rutherford backscattering spectroscopy) with 3.6 MeV $^4He^+$ ions. The pore volumes of powder prepared with CSSQ/tCD mixture were calculated using the Barrett–Joyner–Halenda (BJH) method from adsorption/desorption isotherm curves obtained by nitrogen adsorption method. Surface areas and pore sizes of powder prepared with CSSQ/tCD mixture were calculated by the Brunauer–Emmett–Teller (BET) method from adsorption/desorption isotherm curves obtained by nitrogen adsorption method. Pore structure was investigated by transmission electron microscopy (TEM: Hitachi H9000NA) at 300 kV for the electron transparent cross-section specimens which were prepared by argon ion beam milling technique. Depth-profiled PALS was used to determine the pore size and pore interconnectivity in these thin films. The details of the instrument setup and measurement methods appear elsewhere [10,13]. PALS spectra with 10^7 events were acquired at room temperature with a conventional fast–fast lifetime system with a resolution of 500 ps. The positron beam energy was varied from 1 to 8 keV and the POSFIT program was used for data fitting. The Ps lifetime can be correlated with pore size using the extended Tao–Eldrup model [11].

The dielectric constant was measured at a frequency of 100 kHz using a Mercury CV meter with MIS (metal insulator–semiconductor) structure. The leakage current density was measured by using Keithley 237 source–measure unit and HP4155B, respectively, with a MIS (metal–insulator–semiconductor) structure. In the case of MIS structures, for a top electrode with a diameter of 1 mm, Al metal was deposited by electron beam evaporation method. The leakage current density value is taken at the electric field of 0.4 MV cm^{-1}.

Received: October 29, 2002
Final version: February 2, 2003

[1] A. Corma,. *Chem. Rev*. **1997**, *97*, 2373.
[2] a) C. T. Kresge, M. E. Leonowicz, W. J. Roth, J. C. Vartuli, J. S. Beck, *Nature* **1992**, *359*, 710. b) T. Yanagisawa, T. Shimizu, K. Kuroda, C. Kato, *Bull. Chem. Soc. Jpn*. **1990**, *63*, 988. c) R. Tamaki, Y. Chujo, *J. Mater. Chem* **1998**, *8*, 1113.
[3] a) B.-H. Han, S. Polarz, M. Antonietti, *Chem. Mater.* **2001**, *13*, 3915. b) S. Polarz, B. Smarsly, L. Bronstein, M. Antonietti, *Angew. Chem*. **2001**, *113*, *23*, 4549. c) B.-H. Han, M. Antonietti, *Chem. Mater.* **2002**, *14*, 3477.
[4] a) J. L. Hedrick, R. D. Miller, C. J. Hawker, K. R. Carter, W. Volksen, D. Y. Yoon, M. Trollsas, *Adv. Mater*. **1998**, *10*, 1049. b) C. V. Nguyen, K. R. Carter, C. J. Hawker, J. L. Hedrick, R. L. Jaffe, R. D. Miller, J. F. Remenar, H. W. Rhee, P. M. Rice, M. F. Toney, M. Trollsas, D. Y. Yoon, *Chem. Mater.* **1999**, *11*, 3080. c) S. Mikoshiba, S. Hayase, *J. Mater. Chem.* **1999**, *9*, 591. d) A. T. Kohl, R. Mimna, R. Shick, L. Rhodes, Z. L. Wang, P. A. Kohl, *Electrochem. Solid State Lett.* **1999**, *2*, 77. e) N. Aoi, *Jpn. J. Appl. Phys.* **1997**, *36*, 1355. f) S. Yang, P. A. Mirau, C. Pai, O. Nalamasu, E. Reichmanis, J. C. Pai, Y. S. Obeng, J. Seputro, E. K. Lin, H. Lee, J. Sun, D. W. Gidley, *Chem. Mater.* **2002**, *14*, 369.
[5] A. P. Croft, R. A. Bartsch, *Tetrahedron* **1983**, *39*, 1417.
[6] a) A. Hybl, R. E. Rundle, D. E. Williams, *J. Am. Chem. Soc*. **1965**, *87*, 2779. b) K. Takeo, T. Kuge, *Agric. Biol. Chem*. **1970**, *34*, 1787. c) K. Takeo, T. Kuge, *Agric. Biol. Chem*. **1970**, *34*, 568. d) J. Szejtli, *Cyclodextrin Technology*, Kluwer Academic Publishers, Dordrecht, The Netherlands **1988**, p. 12.
[7] J.-H. Yim, Y.-Y. Lyu, H.-D. Jeong, S. K. Mah, J. Hyeon-Lee, J.-H. Hahn, G. S. Kim, S. Chang., J.-G. Park, *J. Appl. Polym. Sci.*, in press.
[8] C. Y. Wang, Z. X. Shen, J. Z. Zheng, *Appl. Spectrosc.* **2000**, *54*, 209.
[9] C. J. Hawker, J. L. Hedrick, R. D. Miller, W. Volksen, *MRS Bull.* **2000**, *25*, 54.
[10] D. W. Gidley, W. E. Frieze, T. L. Dull, J. Sun, A. F. Yee, C. V. Nguyen, D. Y. Yoon, *Appl. Phys. Lett*. **2000**, *76*, 1282.
[11] T. L. Dull, W. E. Frieze, D. W. Gidley, J. N. Sun, A. F. Yee, *J. Phys. Chem. B* **2001**, *105*, 4657.
[12] S. Lee, J. Yoo, K. Oh, J. Park, *Mater. Res. Soc. Symp. Proc*. **1997**, *476*, 291.
[13] D. W. Gidley, W. E. Frieze, A. F. Yee, T. L. Dull, H.-M. Ho, E. T. Ryan, *Phys. Rev. B: Condens. Matter Mater. Phys.* **1999**, *60*, R5157.

